Tricarballylate Catabolism in *Salmonella enterica*. The TcuB Protein Uses 4Fe-4S Clusters and Heme to Transfer Electrons from $FADH_2$ in the Tricarballylate Dehydrogenase (TcuA) Enzyme to Electron Acceptors in the Cell Membrane†

Jeffrey A. Lewis and Jorge C. Escalante-Semerena*

Department of Bacteriology, University of Wisconsin at Madison, 1550 Linden Drive, Madison, Wisconsin 53706

Received April 6, 2007; Revised Manuscript Received May 25, 2007

ABSTRACT: Tricarballylate, a citrate analogue, is considered the causative agent of grass tetany, a ruminant disease characterized by acute magnesium deficiency. Although the normal rumen flora cannot catabolize tricarballylate, the Gram-negative enterobacterium *Salmonella enterica* can. An operon dedicated to tricarballylate utilization (*tcuABC*) present in this organism encodes all functions required for tricarballylate catabolism. Tricarballylate is converted to the *cis*-aconitate in a single oxidative step catalyzed by the FAD-dependent tricarballylate dehydrogenase (TcuA) enzyme. We hypothesized that the uncharacterized TcuB protein was required to reoxidize the flavin cofactor *in vivo*. Here, we report the initial biochemical characterization of TcuB. TcuB is associated with the cell membrane and contains two 4Fe-4S clusters and heme. Site-directed mutagenesis of cysteinyl residues putatively required as ligands of the 4Fe-4S clusters completely inactivated TcuB function. TcuB greatly increased the V_{max} of the TcuA reaction from 69 ± 2 to 8200 ± 470 nmol min^{-1} mg^{-1}; the K_m of TcuA for tricarballylate was unaffected. Inhibition of TcuB activity by an inhibitor of ubiquinone oxidation, 2,5-dibromo-3-methyl-6-isoproylbenzoquinone (DBMIB), implicated the quinone pool as the ultimate acceptor of electrons from $FADH_2$. We propose a model for the electron flow from $FADH_2$, to the 4Fe-4S clusters, to the heme, and finally to the quinone pool.

Tricarballylate, a citrate analogue, is considered the causative agent of grass tetany, a ruminant disease characterized by acute magnesium deficiency (*1*). Previous reports have found a strong correlation between the accumulation of *trans*-aconitate in the rumen and the incidence of the disease (*2*). In the rumen, *trans*-aconitate is rapidly reduced to tricarballylate (*3*), leading to Mg(II) ion chelation and excretion, and inhibition of aconitase (*1*, *4*, *5*).

Neither the ruminant nor the normal rumen flora can catabolize tricarballylate. However, it was previously reported that *Salmonella enterica* serovar Tymphimurium strain LT2 (hereafter referred to as *S. enterica*) can utilize tricarballylate as a carbon and energy source (*6*). Four genes in this bacterium encode functions required to catabolize tricarballylate (*7*). Three of the tricarballylate utilization (*tcu*) genes, *tcuABC*, comprise a single transcriptional unit, whereas a fourth gene (*tcuR*) is independently transcribed from *tcuABC* (*7*).

We have previously shown that TcuA is an FAD-dependent tricarballylate dehydrogenase that converts tricarballylate to *cis*-aconitate *in vitro* (*8*). Although the function of TcuA is known, and TcuC has been shown to transport citrate across the cell membrane (*7*), the biochemical function of TcuB remained unknown. The primary amino acid sequence of TcuB contained some interesting features. First, TcuB contains two $C\text{-}X_2\text{-}C\text{-}X_2\text{-}C\text{-}X_3\text{-}C$ motifs in its N-terminal half. These motifs are commonly found in proteins containing iron−sulfur clusters (*9*). Second, the C-terminal half of TcuB appears to be very hydrophobic (from residue 112 to the end), suggesting that TcuB may have an integral membrane domain. The predicted topology of TcuB is that the polypeptide contains six transmembrane-spanning domains (*10*).

An appealing hypothesis was that TcuB acted as an electron shuttle protein that reoxidized $FADH_2$ generated by TcuA. Although it has been shown that oxygen can reoxidize the $FADH_2$ *in vitro*, we hypothesized that TcuB was required for efficient reoxidation of the flavin cofactor *in vivo* (*8*).

Here, we report the initial biochemical characterization of TcuB. We show that TcuB contains two 4Fe-4S clusters in its cytosolic N-terminal half and heme in its membrane domain. We present evidence that TcuB is localized to the cell membrane and show that it has a strong positive effect on TcuA activity. On the basis of our data, we suggest that TcuB is an electron-transfer protein that accepts electrons from the reduced flavin cofactor of the tricarballylate dehydrogenase (TcuA) enzyme and releases these electrons to the quinone pools of the membrane using heme as the ultimate electron donor.

MATERIALS AND METHODS

Bacterial Strains, Culture Media, and Growth Conditions. A list of strains and plasmids and their genotypes is provided

† This work was supported by PHS Grant R01 GM62203 to J.C.E.-S. J.A.L. was supported in part by the Department of Bacteriology Jerome Stefaniak Predoctoral Fellowship and by the Molecular Biosciences Training Grant T32 GM07215.

* Corresponding author. Tel: 608-262-7379. Fax: 608-265-7309. E-mail: escalante@bact.wisc.edu.

10.1021/bi7006564 CCC: $37.00
Published on Web 07/14/2007

Table 1: Strain and Plasmid List

strain or plasmid	genotype	reference or source
E. coli		
DH5α/F′	F′/*endA1 hsdR17* (r_k^- m_k^+) *supE44 thi-1 recA1 gyrA* (Na1^r) *relA1* Δ(*lacZYA-argF*)*U169 deoR* [*ϕ*80d*lac*Δ(*lacZ*)*M15*]	New England Biolabs
ER2566	F$^-$ *λ*$^-$ *fhuA2* [*lon*] *ompT lacZ::T7 geneI gal sulA11* Δ(*mcrC-mrr*)*114::IS10 R*(*mcr-73*::miniTn*10*)*2 R*(*zgb-210*::Tn*10*)*1* (Tet^s) *endA1 [dcm]*	New England Biolabs
C43(DE3)	F$^-$ *ompT gal hsdS$_B$* ($r_B^-m_B$) *gal dcm* (DE3)	(*18*)
JE6289	DH5α/ pTCU12 (*bla*$^+$ *tcuA*$^+$ cloned into pTYB1)	Lab Collection
JE7920	DH5α/ pTCU30 (*bla*$^+$ *tcuB*$^+$ cloned into pBAD18s)	
JE8260	DH5α/ pTCU41 (*bla*$^+$ *tcuB42* cloned into pBAD18s, encodes TcuB^{C34A})	
JE8300	DH5α/ pTCU48 (*bla*$^+$ *tcuB47* cloned into pBAD18s, encodes TcuB^{C62A})	
JE8486	DH5α/ pTCU55 (*bla*$^+$ *tcuB*$^+$ cloned into pET15b)	
JE9575	DH5α/ pTCU76 (*bla*$^+$ *tcuB43* cloned into pBAD18s, encodes TcuB^{C38A})	
JE9576	DH5α/ pTCU77 (*bla*$^+$ *tcuB58* cloned into pBAD18s, encodes TcuB^{C68A})	
JE9577	DH5α/ pTCU78 (*bla*$^+$ *tcuB59* cloned into pBAD18s, encodes TcuB^{C72A})	
JE9603	DH5α/ pTCU49 (*bla*$^+$ *tcuB49* cloned into pBAD18s, encodes TcuB^{C31A})	
JE9815	DH5α/ pTCU80 (*bla*$^+$ *tcuB60* cloned into pTEV6 encodes TcuB$^{A115-380}$)	
S. enterica		
TR6583	*metE205 ara-9*	K. Sanderson via J. Roth
derivatives of TR6583		
JE6335	*ybfM106*::MudJ(*kan*$^+$) *tcuB17*	
plasmids		
pTYB1		New England Biolabs
pBAD18s		(*17*)
pET15b		Novagen
pTEV6		Lab Collection

in Table 1. All chemicals were purchased from Sigma unless otherwise stated. *Escherichia coli* cultures were grown in lysogeny broth (LB, (*11*, *12*)). Antibiotic concentrations in rich medium were (in *μ*g/mL) ampicillin (Ap), 100; and kanamycin (Km), 50. Antibiotic concentrations in minimal medium were (in *μ*g/mL) Ap, 100; and Km, 50. No-carbon essential (NCE) medium (*13*) was supplemented with $MgSO_4$ (1 mM), L-methionine (0.5 mM), NH_4Cl (30 mM), and trace minerals (*14*) (*15*). Liquid media contained 20 mM tricarballylate. For growth curves, *S. enterica* strains were grown overnight in LB broth. Two microliters of the overnight cultures was used to inoculate 198 *μ*L of fresh medium in 96-well microtiter dishes. Growth was monitored with an ELx808 high-throughput spectrophotometer **(**Bio-Tek Instruments). Cell density readings at 650 nm were taken every 30 min for 36 h. Cultures were shaken for 1800 s between measurements, and the incubation chamber was maintained at 37 °C. The growth behavior of each strain was analyzed in triplicate.

Recombinant DNA Techniques for Plasmid Construction. Restriction and modification enzymes were purchased from Promega unless otherwise stated and were used according to the manufacturer's instructions. All DNA manipulations were performed in *E. coli* strain DH5α except where noted. Plasmids were transformed into cells by $CaCl_2$ heat shock as described (*16*). Plasmid DNA was isolated by using the Wizard Plus SV Plasmid Miniprep kit from Promega as per the manufacturer's instructions. DNA was isolated from 1% (w/v) agarose gels and purified by using the Qiaquick Gel Extraction kit (QIAGEN). PCR products were purified by using the Qiaquick PCR purification kit (QIAGEN) as per manufacturer's instructions. DNA was sequenced using Big Dye protocols and resolved at the Biotechnology Center at the University of Wisconsin—Madison. Genomic DNA for PCR was prepared from *Salmonella enterica* strain TR6583 (*metE205 ara-9*) using the MasterPure genomic DNA purification kit (Epicenter Technologies). All primers used for PCR amplifications were purchased from Integrated DNA Technologies.

Overproduction and Purification of TcuA Protein. TcuA protein was purified and reconstituted with FAD as described (*8*).

Overproduction of H_6TcuB-Enriched Cell-Free Extract. *S. enterica* H_6TcuB protein was overproduced using plasmid pTCU55 in *E. coli* strain C43 (*17*). Ten milliliters of an overnight culture of *E. coli* C43/pTCU55 grown at 37 °C in LB containing ampicillin was used to inoculate 1 L of terrific broth (TB) (*18*) supplement with $FeCl_3$ (10 *μ*M), cysteine (0.3 M), and ampicillin (100 *μ*g/mL). TB cultures were grown at 18 °C with shaking to a cell density (optical density at 600 nm) of 0.4, at which point isopropyl-*β*-D-thiogalactopyranoside (IPTG) was added to a final concentration of 300 *μ*M. After the addition of IPTG, cultures were incubated under the same conditions for an additional 18 h. Cells were

harvested by centrifugation at 7,741*g* at 4 °C for 10 min using an Avanti J-20 XPI centrifuge (Beckman-Coulter) equipped with a JLA 8.1000 rotor. Cells were resuspended in tris(hydroxymethyl)aminomethane buffer (Tris-HCl) (100 mM, pH 7.5 at 25 °C) supplemented with 1 mL of Protease Inhibitor Cocktail (Sigma). Cells were broken by passing them four times through a French press (Aminco) at 1.6×10^5 kPa using a 40-mL chilled pressure cell. Unbroken material and cell debris were removed by centrifugation at 5000*g* for 10 min at 4 °C. The supernatant was centrifuged at 75,600*g* for 90 min. The membrane pellet was resuspended in Tris-HCl buffer (100 mM, pH 7.5 at 25 °C) and homogenized using a Dounce homogenizer (Fisher). Homogenized membrane material was diluted to 10 mg/mL, and a 200-mM solution of 1,2-diheptanoyl-*sn*-phosphatidylcholine (DHPC, Avanti Polar Lipids) (*19*) (*20*) was added dropwise to a final concentration of 15 mM. Membrane material was incubated with DHPC on ice for 30 min and centrifuged at 75,600*g* for 30 min at 4 °C, and the H_6-TcuB-enriched supernatant was saved. Glycerol was added at 20% (v/v), and the H_6-TcuB-enriched membrane extract was flash-frozen in liquid N_2 and stored at −80 °C until used.

Purification of H_6TcuB. Cells overproducing H_6TcuB protein were grown as described above. Detergent-solubilized membrane extract was prepared as described above, except that after cell breakage, all steps were performed in an anoxic chamber (Coy), and all buffers used were sparged with O_2-free N_2 for 30 min prior to use. H_6TcuB protein was purified using His·Bind Resin (Novagen), as per manufacturer's instructions. Protein was eluted with buffer A (Tris-HCl (20 mM) at pH 7.9 at 25 °C, NaCl (0.5 M), glycerol (20% v/v), and imidazole (1.0 M)). Fractions containing H_6TcuB were pooled and concentrated using a Centriprep YM-10 centrifugal filter (Amicon), as per manufacturer's instructions. After concentration, the protein was desalted to remove any nickel that leached from the resin during purification using a 5-mL HiTrap Desalting column (Amersham). This was performed using a syringe, as per manufacturer's specifications, except that the column was equilibrated using buffer that was sparged with O_2-free N_2 for 30 min. The protein was eluted with buffer A. Protein purity was assessed by sodium dodecyl sulfate−polyacrylamide-gel electrophoresis (SDS−PAGE) (*21*) after staining with Coomassie Brilliant Blue R-250 (*22*). Western blots were performed using anti-His_5 Tag monoclonal antibodies (Novagen) as per manufacturer's instructions. Protein concentration was determined as described (*23*). Purified H_6TcuB protein (92% homogeneous) was dispensed into serum vials fitted with rubber stoppers and frozen at −80 °C for storage until use.

Purification of MBPH_6TcuB$^{\Delta 115-380}$. The peptide comprising the first 114 amino acid residues of TcuB (TcuB$^{\Delta 115-380}$) was overproduced with both a maltose-binding protein (MBP) and a hexa-histidine tag fused to its N-terminus using plasmid pTCU80 in *E. coli* strain C43. Overproduction conditions were the same for H_6TcuB. Cells were harvested as described for H_6TcuB. Following harvest, all steps were performed in an anoxic chamber (Coy), and all buffers used were sparged with O_2-free N_2 for 30 min prior to use. Cells were broken by resuspension in buffer containing Tris-HCl buffer (20 mM) at pH 7.9, NaCl (1.0 M), imidazole (5 mM), lysozyme (1 mg/mL), and Bug Buster (Novagen). Broken cells were centrifuged at 30,000*g* for 30 min at 4 °C to remove cell debris. MBPH_6TcuB$^{\Delta 115-380}$ was purified using His·Bind Resin (Novagen), as per manufacturer's instructions. Protein was eluted with Tris-HCl buffer (20 mM, pH 7.9 at 25 °C) containing NaCl (0.5 M) and imidazole (1.0 M). Glycerol was added (20% v/v), and the protein was desalted as with H_6TcuB above. Purified MBPH_6TcuB$^{\Delta 115-380}$ protein (60% homogeneous) was dispensed into serum vials fitted with rubber stoppers and frozen at −80 °C for storage until use.

In-Gel Heme-Dependent Peroxidase Assay. To test for the presence of heme in H_6TcuB, we used both a colorimetric in-gel heme peroxidase assay that consisted of H_2O_2, the hydrogen donor dimethoxybenzidene (DMB, or *o*-dianisidine) (*24*), and the chemiluminescent detection system. For the colorimetric detection-based assay, H_6TcuB protein (3 μg), horse heart cytochrome *c* (3 μg; positive control for hemoprotein), and bovine serum albumin (10 μg; negative control) were loaded onto a 12% (w/v) polyacrylamide separation phase with a 5% polyacrylamide stacker layer. The heme peroxidase assay procedure was as described (*24*) with the following modifications. The polyacrylamide gel electrophoresis running buffer consisted of Trizma base (25 mM), glycine (192 mM), and sodium dodecyl sulfate (SDS) (0.1% w/v) with no pH adjustment. The sample preparation buffer was the Non-Reducing Lane Marker Sample Buffer (Pierce), which consisted of Tris-HCl buffer (60 mM, pH 6.8), SDS (1% w/v), glycerol (10% v/v), and a proprietary tracking dye. DMB was dissolved in 20 mL of glacial acetic acid and then mixed with 160 mL of ddH_2O. The rest of the staining procedure was as described (*24*). Following staining with H_2O_2 and DMB, the polyacrylamide gel was stained with Coomassie Brilliant Blue R-250 (*22*) to identify bands that did not contain heme. For chemiluminescent detection, H_6TcuB protein (6 μg), horse heart cytochrome *c* (1 μg; positive control for hemoprotein), and bovine serum albumin (10 μg; negative control) were separated via SDS−PAGE as described above and transferred to a PVDF membrane (Millipore) as per manufacturer's instructions. The membrane was incubated with SuperSignal West Dura Extended Duration Substrate (Pierce) as per manufacturer's instructions and exposed to X-ray film for 5 min before development.

EPR Spectroscopy of H_6TcuB and MBPH_6TcuB$^{\Delta 115-380}$. Samples of TcuB (22 μM), MBP H_6TcuB$^{\Delta 115-380}$ (81 μM), or a pTEV6 vector-only control (81 μM) were either opened to the air (referred to as oxidized) or incubated with sodium dithionite (10 mM) for 20 min before freezing anaerobically with liquid N_2-cooled isopentane. EPR spectra were recorded at 10 K using a Varian spectrometer with an Oxford ESR-900 continuous flow liquid He cryostat.

Redox Potentiometry of H_6TcuB. Spectroelectrochemical titrations were performed at 25 ± 2 °C inside an anoxic chamber (Coy). The redox mediators used included methyl viologen ($E_o' = -0.446$ mV; 0.3 μM), benzyl viologen ($E_o' = -0.359$ mV; 1 μM), phenazine methosulfate ($E_o' = 0.08$ mV; 1 μM), triphenyltetrazolium ($E_o' = -0.08$ mV; 1 μM), quinhydrone ($E_o' = 0.285$ mV; 1 μM), 2,6-dichlorophenolindolphenol ($E_o' = 0.217$; 1 μM), and methylene blue (μM). H_6TcuB (4.6 μM in buffer A) was titrated electrochemically according to the method of Dutton (*25*) using sodium dithionite as reductant. Oxidative titrations with potassium ferricyanide could not be performed because H_6TcuB was unstable under the conditions used. Absorption spectra (300−

700 nm) of 100 μL samples in a 96-well microtiter plate were recorded using a Powerwave XS spectrophotometer (Biotek Instruments). The electrochemical potential was monitored using a 6230N pH Meter coupled to an ORP-146C Pt/AgCl combination electrode (Lazar). The electrode was calibrated using saturated quinhydrone at pH 7.0 (E_m = 285 mV) and pH 4.0 (E_m = 462 mV). The observed potentials were relative to the KCl saturated AgCl reference, and these were corrected to values relative to the standard hydrogen electrode (SHE) by the addition of 199 mV to the data obtained by the Pt/AgCl electrode. The absorbance change at 425 nm was used to determine the concentration of oxidized and reduced TcuB. Redox mediators did not appreciably absorb at this wavelength throughout the course of the titration. Data were plotted in GraphPad Prism version 4 as E_{obs} versus log([oxidized]/[reduced]). Using this plot, the midpoint potential of the half-reaction can be determined using the Nernst equation: $E_{obs} = E_m + 2.303(RT/nF)$log([oxidized]/[reduced). At 25 °C, the slope of the line is 0.059, and the *y*-intercept is the midpoint potential in V.

Optimal Parameters for Assaying H_6TcuB Electron Transfer. cis-Aconitate production was quantified using a described HPLC protocol (*8*). Optimal tricarballylate dehydrogenase activity was measured in reaction mixtures (200-μL final volume) that contained TcuA protein (95% homogeneous, 1 μg), dithiothreitol (DTT; 1 mM), and Tris-HCl buffer (100 mM, pH 7.5 at 30 °C). Reaction mixtures were preincubated for 5 min at 30 °C prior to the addition of tricarballylate (10 mM). Increasing amounts of H_6TcuB-enriched cell-free extract (1 μg to 100 μg) were added. Cell-free extract (20 μg of protein) obtained from cells carrying empty pET15b cloning vector was used as control. Product formation was quantified after a 10-min incubation period.

Optimal pH. 2-Morpholinoethanesulfonic acid (MES) or Tris-HCl buffer (100 mM) was used to determine the optimal pH for assaying tricarballylate dehydrogenase activity. All buffer solutions had their pH adjusted at 30 °C. MES was used as buffer in reaction mixtures where the pH value was 6.5 and below. Tris-HCl buffer was used in reaction mixtures where the pH was 7.0 and above. After the addition of tricarballylate (10 mM), 40-μL samples were removed after 3, 6, and 9 min of incubation at 30 °C and added to 60-μL of sulfuric acid (167 mM). Samples (50-μL) were analyzed by HPLC as described (*8*). The optimal pH for TcuA activity in the absence of H_6TcuB was determined as described (*8*). All reactions were performed in triplicate.

Optimal Temperature. After finding an apparent pH optimum for H_6TcuB enhanced tricarballylate dehydrogenase activity, the optimal temperature was determined. Assays were performed at 25, 30, 37, and 45 °C using MES buffer (100 mM) at pH 6.5 at each temperature assayed. After the addition of tricarballylate (10 mM), 40-μL samples were removed after 3, 6, and 9 min of incubation at 30 °C and added to 60 μL of sulfuric acid (167 mM). Samples (50-μL) were analyzed by HPLC as described (*8*). All reactions were performed in triplicate. The optimal temperature for TcuA activity in the absence of H_6TcuB was determined as described (*8*). All reactions were performed in triplicate.

Kinetic Parameters. Optimal conditions were used to assay TcuA activity as a function of substrate concentration in both the presence and absence of H_6TcuB extract. The range of tricarballylate concentrations analyzed was between 0.1 and 10 mM. For reactions containing H_6TcuB extract, 40-μL samples were removed at 1, 2, and 3-min intervals following the addition of tricarballylate. For reactions containing only TcuA, 40-μL samples were removed after 30 min following the addition of tricarballylate. Samples were added to 60-μL of 167 mM sulfuric acid to give a final sulfuric acid concentration of 100 mM. Samples (50-μL) were analyzed by HPLC as described (*8*).

H_6TcuB Inhibition. Optimal conditions were used to assay TcuA activity in either the presence or the absence of H_6-TcuB-enriched cell-free extract. After the addition of tricarballylate (10 mM) to the reaction mixture, 40-μL samples were removed at either 10 or 60 min for samples that did or did not contain H_6TcuB extract, respectively. Samples were added to 60 μL of sulfuric acid (167 mM) to give a final sulfuric acid concentration of 100 mM. Fifty microliters of the samples were injected and developed using the HPLC method as described (*8*). Inhibitors used were potassium cyanide (KCN; 100 μM and 1 mM), 2,5-dibromo-3-methyl-6-isopropyl-*p*-benzoquinone (DBMIB; 100 μM and 1 mM), and bathophenanthroline (Bth; 10 μM and 100 μM). DBMIB was dissolved in ethanol, thus the control treatment for TcuA activity included 2% (v/v) ethanol.

Metal Analysis. TcuA (20 μM) was dialyzed overnight into buffer containing *N*-cyclohexyl-2-aminoethanesulfonic acid (HEPES; 20 mM) at pH 7.5 at 4 °C and tris(2-carboxyethyl)-phosphine (TCEP; 0.25 mM). Samples containing TcuA and a buffer control were analyzed for bound metal ions by inductively coupled plasma emission spectrometry (ICPES; Chemical Analysis Laboratory, University of Georgia) by using a Thermo Jarrell-Ash 965 (New Port Richey, FL) inductively coupled argon plasma spectrophotometer. For TcuB and MBPH_6TcuB$^{\Delta 115-380}$, samples were concentrated by using a Centriprep YM-10 centrifugal filter (Amicon), as per manufacturer's instructions, and the flow through was used as a buffer control. This was done to avoid the precipitation that occurred during dialysis. TcuB (11 μM) and MBPH_6TcuB$^{\Delta 115-380}$ (27 μM) were analyzed for bound metals by ICPES (Soil and Plant Analysis Lab, University of Wisconsin Madison) by using a Thermo Jarrell-Ash IRIS Advantage inductively coupled argon plasma spectrophotometer.

RESULTS

TcuB Protein Contains Heme. We used plasmid pTCU55 to overproduce H_6TcuB protein, which was purified under anoxic conditions using nickel affinity chromatography. Membrane preparations enriched with H_6TcuB had a deep-red color. Membrane preparations obtained from cells carrying the empty cloning vector used to overproduce H_6-TcuB were colorless. Purified H_6TcuB protein (≥92% homogeneous, Figure 1) was red. Purified H_6TcuB protein had an apparent molecular mass of 35 kDa on the basis of SDS−PAGE compared to a predicted mass of 42 kDa. Western blots using anti-His Tag monoclonal antibodies detected a single band at 35 kDa in both cell lysates and purified H_6TcuB (data not shown). The EPR spectrum of purified H_6TcuB exposed to air contained signals consistent with the presence of low-spin heme (Figure 2A.) The measured *g*-values of $g_z = 2.96$, $g_y = 2.28$, and $g_x = 1.85$ correspond to those reported for other proteins with a low-

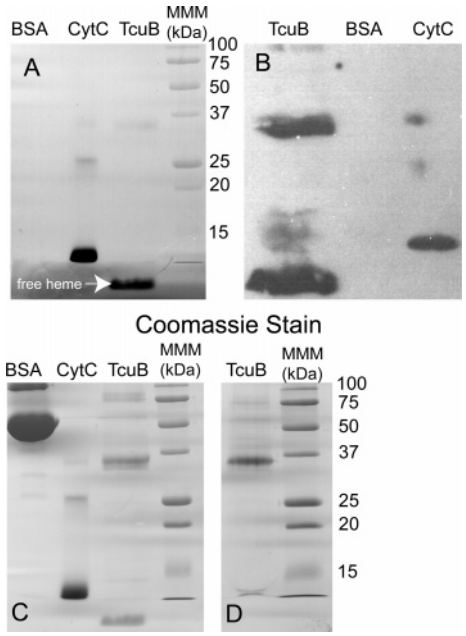

FIGURE 1: SDS−PAGE of purified TcuB and stain for hemoproteins. (A) Purified H_6TcuB (3 μg, 42 kDa) was stained with a double-staining process that specifically stains heme. Cytochrome *c* (3 μg, 12 kDa) was used as a positive control, and bovine serum albumin (BSA, 10 μg, 92 kDa) was used as a negative control. (B) More sensitive heme peroxidase detection using a chemiluminescent substrate (Pierce). H_6TcuB (6 μg, 42 kDa), bovine serum albumin (BSA, 10 μg, 92 kDa), and cytochrome *c* (1 μg, 12 kDa). (C) Same as that in A after staining with Coomassie Brilliant Blue. (D) H_6-TcuB (2 μg) stained with only Coomassie to assess purity.

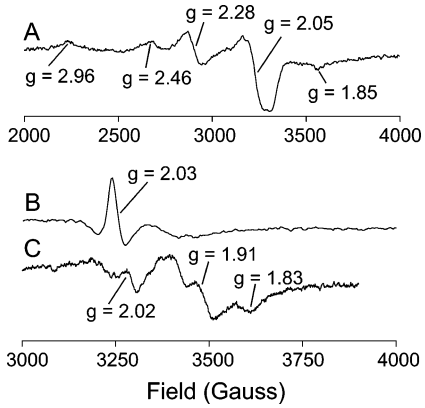

FIGURE 2: EPR spectroscopy of H_6TcuB and $MBPH_6TcuB^{\Delta 115-380}$. Oxidized full-length H_6TcuB (A), oxidized $MBPH_6TcuB^{\Delta 115-380}$ (B), and dithionite reduced $MBPH_6TcuB^{\Delta 115-380}$ (C).

spin heme (*26*). We were unable to account for the *g*-value at $g = 2.46$, and hypothesize that it may be free heme that dissociated during handling of the protein. The UV−visible absorbance spectrum of purified H_6TcuB was dominated by a Soret band characteristic of heme cofactors (Figure 3). The presence of heme in the H_6TcuB protein was confirmed by in-gel, heme-dependent peroxidase activity assays. Results from these assays indicated that the heme cofactor was not covalently attached to the protein because the bulk of the heme migrated with the dye front (Figure 1A). More sensitive chemiluminescent detection verified that some heme remains associated with H_6TcuB (Figure 1B). Purified H_6TcuB protein lacking the last 266 amino acid residues comprising the membrane domain lacked the Soret band suggesting that

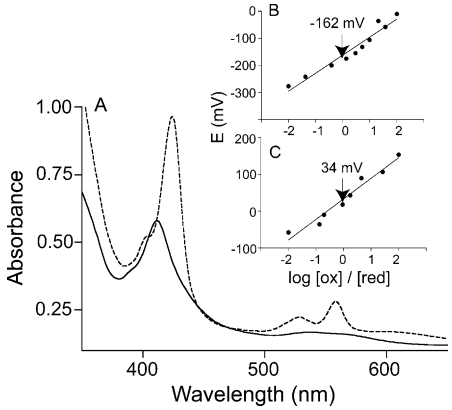

FIGURE 3: Redox potentiometry of H_6TcuB protein. The absorbance spectrum of H_6TcuB as purified (oxidized, solid lines) and dithionite reduced (dotted lines). Inset B shows a plot for the more electronegative species of potential data versus log[H_6TcuB oxidized]/[H_6TcuB reduced]. The *y*-intercept indicates the midpoint potential of −162 mV for H_6TcuB. Inset C shows a plot for the more positive species of the potential data vs log[H_6TcuB oxidized]/[H_6TcuB reduced]. The *y*-intercept indicates the midpoint potential of 34 mV for what we propose is the dissociated heme.

the membrane domain housed the heme cofactor (data not shown).

TcuB Contains Two 4Fe-4S Clusters. TcuB contains two cysteine-rich motifs characteristic of proteins with 4Fe-4S clusters (*9*). Acidification of the protein created a distinct rotten-egg odor suggestive of acid-labile sulfur found in Fe−S clusters. The EPR spectrum of both purified full-length H_6TcuB and $MBPH_6TcuB^{\Delta 115-380D}$ protein provided evidence for 4Fe-4S clusters. The EPR spectrum of oxidized H_6TcuB contained a signal consistent with a 4Fe-4S cluster in the +3 oxidation state (*27*) (Figure 2B). The *g*-value of 2.05 was in excellent agreement with the reported *g*-values for other $[4Fe\text{-}4S]^{+3}$ clusters (*27*). However, the assignment of the peaks in the spectrum was complicated by the presence of at least one heme species as described above. The EPR spectrum of oxidized $MBPH_6TcuB^{\Delta 115-380}$, a variant that lacks the predicted membrane domain, contained a signal ($g = 2.03$) consistent with a 3Fe-4S cluster (Figure 3B) as well as considerable amounts of free iron. Free iron was only detected in spectra from oxidized protein, which was consistent with the breakdown of 4Fe-4S clusters to 3Fe-4S clusters because of oxidative damage. The EPR spectrum of variant $MBPH_6TcuB^{\Delta 115-380}$ protein reduced with dithionite contained multiple signals at $<2.0g$ which were consistent with reduced 4Fe-4S clusters (Figure 3C). The EPR spectrum from purified vector-only control protein extract did not contain any signals consistent with any type of iron−sulfur cluster (data not shown). Metal analysis was performed on both the full-length H_6TcuB and $MBPH_6TcuB^{\Delta 115-380}$ variant to determine the molar quantities of iron and sulfur. The results indicated that H_6TcuB contained 12.4 mol S and 6 mol Fe per mol of protein, whereas $MBPH_6TcuB^{\Delta 115-380}$ contained 5.6 mol S and 1.7 mol Fe per mol of protein, which suggested that both proteins contained substoichiometric amounts of their metal cofactors.

To determine whether the putative cysteine-rich motifs were required for *tcuB* function, alanine substitutions were made in the cysteines of each motif; C31, C34, and C38 for the first cluster, and C62, C68, and C72 for the second. Mutant alleles were tested for the ability to complement a

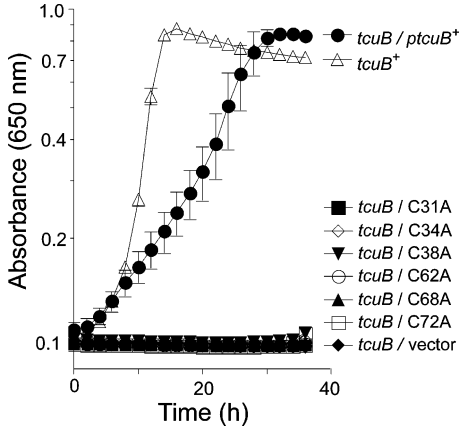

FIGURE 4: Mutations in the conserved cysteines of TcuB cannot complement a *tcuB* mutant. Cells were grown aerobically in NCE medium containing tricarballylate (20 mM) and 500 μM arabinose to induce the expression of the cloned genes. *tcuB* refers to allele *tcuB17*, *tcuB*$^+$ refers to strain TR6583, vector refers to the pBAD18s cloning vector, and C31A−C72A refer to the amino acid substitution of TcuB on the plasmid. The error bars denote standard error.

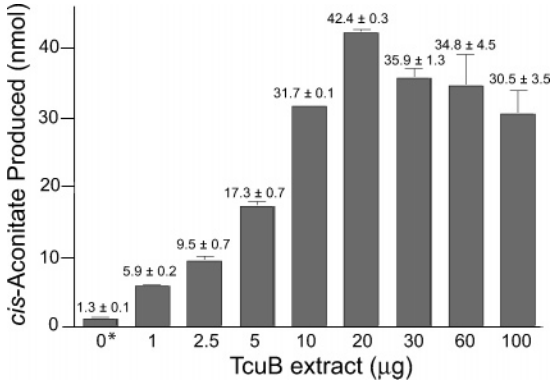

FIGURE 5: Titration of TcuB for TcuA activity assays. The bars show the amount of *cis*-aconitate produced in 10 min with 1 μg of TcuA and varying amounts of TcuB-containing extract. The asterisk for 0 μg of TcuA denotes that 20 μg of extract from cells containing an empty vector were used as a control. Error measurements are presented as standard error.

chromosomal *S. enterica tcuB* missense mutant (strain JE6335). None of the mutant alleles restored growth on tricarballylate after 36 h (Figure 4), which provided support for the idea that the cysteine residues tested were necessary for protein function. Although we cannot exclude the possibility that the cysteine residues are merely structurally important, these results were consistent with the cysteines being ligands for 4Fe-4S clusters. Variant proteins were unstable and could not be isolated, and consequently, no EPR spectra were obtained.

Redox potentiometry of H_6TcuB was performed to determine the midpoint potential for the heme cofactor of the protein. Reduction of the protein with dithionite red-shifted the Soret band from 412 to 425 nm, together with the appearance of a peak at 556 nm (Figure 2). The results showed the presence of two heme species in solution, as indicated by the biphasic nature of the curve (data not shown); protein precipitation was observed throughout the titration, which suggested that one of the heme species seen in the titration was artifactual. Shown in Figure 2B is the titration curve for the more electronegative species ($E_m = -162 \pm 7$ mV). The more electropositive species had a midpoint potential of 34 ± 6 mV (Figure 2C).

TcuB Enhances the Activity of TcuA. The observation that TcuB contained two 4Fe-4S clusters and heme suggested that TcuB was an electron-transfer protein. Because *tcuB* function is required *in vivo* for *S. enterica* to grow on tricarballylate (*7*), we hypothesized that the role of TcuB was to reoxidize the $FADH_2$ electron carrier of TcuA. To test this idea, TcuA tricarballylate dehydrogenase activity was measured with varying amounts of H_6-TcuB-enriched cell-free extract. At saturating levels of H_6-TcuB, the amount of TcuA product (*cis*-aconitate) produced per min was 32.5-fold higher than the control experiment that lacked H_6-TcuB protein (Figure 5).

Reassessment of TcuA Kinetic Parameters as a Function of H_6-TcuB. pH and temperature optima for tricarballylate dehydrogenase activity were determined in the presence of saturating amounts of H_6-TcuB. Previously, optimal activity for TcuA was shown to occur within a pH between 7.0 and 7.5 with a temperature optimum near 30 °C (*8*). To test whether H_6-TcuB affected these values, the pH and temperature profiles of TcuA with and without H_6-TcuB were reassessed (Tables 2and 3). The addition of H_6-TcuB did not appear to appreciably affect the pH optimum of TcuA. However, in the presence of H_6-TcuB, TcuA activity had a lower temperature optimum, the significance of which is unknown.

Table 2: pH Profile for TcuA Alone and with TcuB

	tricarballylate dehydrogenase activity (nmol min^{-1} mg^{-1})	
pH	−TcuB	+TcuB
6.0	60 ± 3	4700 ± 100
6.5	72 ± 7	9400 ± 100
7.0	67 ± 4	7600 ± 400
7.5	62 ± 1	4600 ± 300
8.0	44 ± 0.1	1500 ± 100

Table 3: Temperature Profile for TcuA Alone and with TcuB

	tricarballylate dehydrogenase activity (nmol min^{-1} mg^{-1})	
temperature (°C)	−TcuB	+TcuB
25	66 ± 6	11800 ± 600
30	83 ± 3	9400 ± 100
37	108 ± 6	10100 ± 100
45	ND	610 ± 20

Kinetic parameters for TcuA were re-evaluated in the presence of H_6-TcuB under optimized pH and temperature conditions (Figure 6). Tricarballylate dehydrogenase activity assays were performed at pH 6.5 at 25 °C. The K_m of TcuA for tricarballylate at pH 6.5 increased almost an order of magnitude compared to the values reported for that at pH 7.5 (*8*). The presence of H_6-TcuB did not change the K_m of TcuA for tricarballylate. However, the velocity of the TcuA reaction increased by over 2 orders of magnitude in the presence of H_6-TcuB. The kinetic parameters for TcuA in the presence and absence of H_6TcuB are presented in Table 4.

Inhibition Studies of TcuB. The H_6TcuB-mediated enhancement of TcuA activity was subjected to various inhibitors to help address whether the cofactors of TcuB are necessary for TcuB activity (Figure 7). Potassium cyanide, a known inhibitor of hemoproteins (*28*), inhibited TcuA

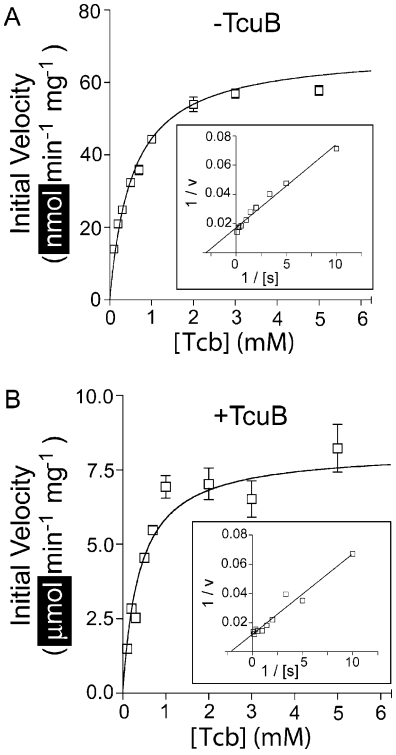

FIGURE 6: Kinetic parameters of TcuA alone and with TcuB. (A) Plot of initial velocity vs tricarballylate concentration for TcuA alone. Initial velocities were calculated by measuring product formation after a 30-min reaction. The error bars denote standard error. The inset shows a Lineweaver−Burk plot of the data. (B) Plot of initial velocity versus tricarballylate concentration for TcuA in the presence of TcuB-enriched extract (20 μg). Initial velocities were calculated by measuring *cis*-aconitate formation at 3-min intervals over a 9-min reaction. The error bars denote standard error. The inset shows a Lineweaver−Burk Plot.

Table 4: Kinetic Parameters

parameter	TcuA	TcuA + TcuB
K_m (mM)	0.6 ± 0.1	0.4 ± 0.1
V_{max} (nmol min^{-1} mg^{-1})	69 ± 2	8200 ± 470
k_{cat} (s^{-1})	5.8×10^{-2}	6.9
k_{cat}/K_m (M^{-1} s^{-1})	1.1×10^{5}	1.8×10^{7}

activity in the presence of H_6TcuB by 67% at 1 mM, whereas TcuA by itself was not inhibited at all. Bathophenanthroline (Bth), an iron chelator (*29*), inhibited TcuA activity in the presence of H_6TcuB by 80% at 100 μM. TcuA was also inhibited by 100 μM Bth, but to a lesser extent (40%). Metal analysis of TcuA showed 0.1 mol of both Ca and Zn per mol of TcuA, with no iron detected (data not shown). TcuA activity remained unchanged with the addition of 1- or 2-fold molar excess of either $CaCl_2$ or $ZnCl_2$ (data not shown). 2,5-Dibromo-3-methyl-6-isoproylbenzoquinone (DBMIB), an inhibitor of ubiquinone oxidation in succinate dehydrogenase and cytochrome *bd* (*30*), was tested to determine if the quinone pool accepted electrons from the heme group of TcuB. DBMIB (1 mM) strongly inhibited TcuA activity in the presence of H_6TcuB (98%) compared to just 23% for TcuA alone.

DISCUSSION

Here, we describe the initial biochemical and functional characterization of TcuB protein of *S. enterica*. Previous

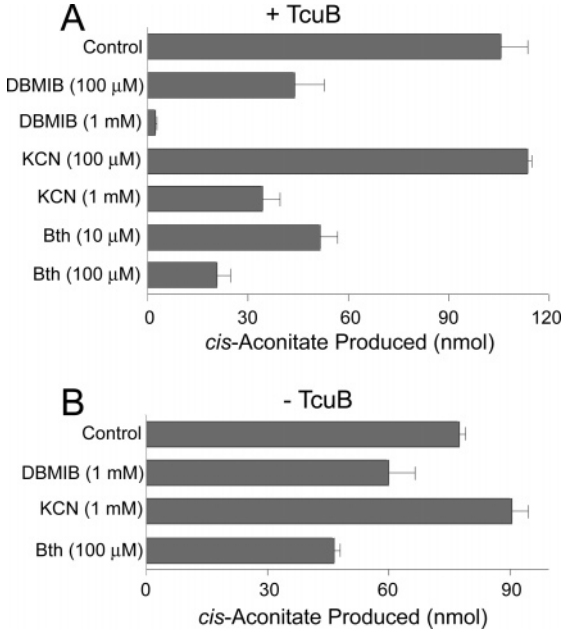

FIGURE 7: Inhibition studies of TcuB. (A) Amount of *cis*-aconitate produced in 10 min by TcuA (1 μg) in the presence of TcuB-enriched extract (20 μg) and various inhibitors. Error measurements are presented as standard error. (B) Amount of *cis*-aconitate produced in 60 min by TcuA (20 μg) in the absence of TcuB. Control, treatment of 2% (v/v) ethanol; DBMIB, 2,5-dibromo-3-methyl-6-isoproylbenzoquinone; KCN, potassium cyanide; Bth, bathophenanthroline.

biochemical characterization of TcuA found that the enzyme converted tricarballylate to *cis*-aconitate and was thus the only catabolic function required to convert tricarballylate into a common metabolic intermediate. We also noted that *in vitro* TcuA had a low V_{max} for a catabolic enzyme. The biochemical characterization of TcuB fills an important gap in our understanding of tricarballylate catabolism. The fact that TcuB improves the V_{max} for TcuA by >100× *in vitro* explains why a *tcuB* mutant cannot grow on tricarballylate despite having the necessary catabolic enzyme (TcuA) to convert tricarballylate to *cis*-aconitate.

We propose that the 4Fe-4S clusters and heme of TcuB serve as cofactors for facilitating the transfer of electrons from the $FADH_2$ group of TcuA to the quinone pool of the cytoplasmic membrane. Tricarballylate growth defects of mutants in the two conserved cysteine motifs support the hypothesis that these cysteines are ligands for 4Fe-4S clusters, although it cannot be ruled out that mutations are only affecting protein structure or stability. The absence of TcuB antibodies for Western blotting leaves this an outstanding question. The diagnostic Soret band of TcuB and a double-stain for hemoproteins provides strong evidence that TcuB contains noncovalent heme. The amino acid sequence for TcuB does not contain a C-X-X-C-H motif consistent with *c*-type cytochromes, thus TcuB is more likely to contain a *b*-type heme. Although a second heme species was detected during redox potentiometry, we interpret this species to be an artifact due to the precipitation of the protein over the course of the experiment. The relatively high redox potential of the second heme species would seem to preclude it from participating in electron transfer from iron−sulfur centers or the other heme to the quinone pool.

The pathway of reoxidation of $FADH_2$ via Fe−S clusters and heme by TcuA and TcuB seems analogous conceptually

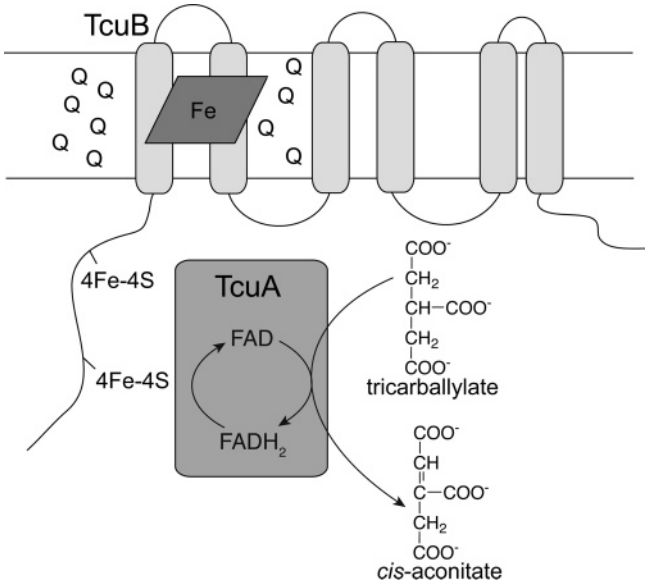

FIGURE 8: Model for tricarballylate catabolism in *S. enterica*. TcuA oxidizes tricarballylate to *cis*-aconitate, which can then be catabolized via the Krebs cycle. We propose that TcuB is an electron shuttle protein responsible for oxidizing $FADH_2$ back to FAD in TcuA.

to the succinate dehydrogenase complex. In fact, TcuA shares sequence similarity with SdhA, and tricarballylate is similar in structure to succinate (differing by a methylcarboxyl group). However, TcuB shares no homology with SdhB, SdhC, or SdhD. SdhB contains one 2Fe-2S cluster, one 3Fe-4S cluster, and one 4Fe-4S cluster, whereas TcuB appears to contain two 4Fe-4S clusters. It is probable that TcuB evolved separately.

For TcuB to continue to reoxidize the $FADH_2$ from TcuA, the electrons need to be passed from the iron−sulfur clusters and the heme into an electron sink. Redox potentiometry studies of TcuB were complicated by the presence of free heme. However, we interpret the more electronegative species to be TcuB. The midpoint potential for TcuB would fall between that of 4Fe-4S clusters and quinones, suggesting that the heme links electrons from the Fe−S clusters to the quinone pool (Figure 8).

Our model shows electrons traveling from $FADH_2$ to the two 4Fe-4S clusters, then to heme, and ultimately to the quinone pool. The use of a known inhibitor of ubiquinol oxidation, DBMIB, showed that TcuA activity in the presence of the H_6-TcuB extract was markedly decreased, strongly suggesting that the quinone pool is required for efficient oxidation of TcuA $FADH_2$.

ACKNOWLEDGMENT

We thank Dr. Susan Wang for her assistance with the acquisition of EPR spectra. We thank Dr. George Reed for lending his expertise on the interpretation of the EPR data and for the use of his EPR spectrometer.

REFERENCES

1. Russell, J. B., and Forsberg, N. (1986) Production of tricarballylic acid by rumen microorganisms and its potential toxicity in ruminant tissue metabolism, *Br. J. Nutr. 56*, 153−162.
2. Burau, R., and Stout, P. R. (1965) trans-Aconitic acid in range grasses in early spring, *Science 150*, 766−767.
3. Russell, J. B. (1985) Enrichment and isolation of rumen bacteria that reduce trans-aconitate to tricarballylic acid, *Appl. Environ. Microbiol. 49*, 120−126.
4. Schloss, J. V., Emptage, M. H., and Cleland, W. W. (1984) pH profiles and isotope effects for aconitase from *Saccharomycopsis lipolytica*, beef heart, and beef liver. α-methyl-*cis*-aconitate and threo-D_s-α-methylisocitrate as substrates, *Biochemistry 23*, 4572−4580.
5. Schwartz, R., Topley, M., and Russell, J. B. (1988) Effect of tricarballylic acid, a nonmetabolizable rumen fermentation product of trans-aconitic acid, on Mg, Ca and Zn utilization of rats, *J. Nutr. 118*, 183−188.
6. Gutnick, D., Calvo, J. M., Klopotowski, T., and Ames, B. N. (1969) Compounds which serve as the sole source of carbon or nitrogen for *Salmonella typhimurium*, *J. Bacteriol. 100*, 215−219.
7. Lewis, J. A., Horswill, A. R., Schwem, B. E., and Escalante-Semerena, J. C. (2004) The tricarballylate utilization (*tcuRABC*) genes of *Salmonella enterica* serovar Typhimurium LT2, *J. Bacteriol. 186*, 1629−1637.
8. Lewis, J. A., and Escalante-Semerena, J. C. (2006) The FAD-dependent tricarballylate dehydrogenase (TcuA) enzyme of *Salmonella enterica* converts tricarballylate into *cis*-aconitate, *J. Bacteriol. 188*, 5479−5486.
9. Jung, Y. S., Bonagura, C. A., Tilley, G. J., Gao-Sheridan, H. S., Armstrong, F. A., Stout, C. D., and Burgess, B. K. (2000) Structure of C42D Azotobacter vinelandii FdI. A Cys-X-X-Asp-X-X-Cys motif ligates an air-stable [4Fe-4S]2+/+ cluster, *J. Biol. Chem. 275*, 36974−36983.
10. von Heijne, G. (1992) Membrane protein structure prediction. Hydrophobicity analysis and the positive-inside rule, *J. Mol. Biol. 225*, 487−494.
11. Bertani, G. (1951) Studies on lysogenesis. I. The mode of phage liberation by lysogenic *Escherichia coli*, *J. Bacteriol. 62*, 293−300.
12. Bertani, G. (2004) Lysogeny at mid-twentieth century: P1, P2, and other experimental systems, *J. Bacteriol. 186*, 595−600.
13. Berkowitz, D., Hushon, J. M., Whitfield, H. J., Jr., Roth, J., and Ames, B. N. (1968) Procedure for identifying nonsense mutations, *J. Bacteriol. 96*, 215−220.
14. Balch, W. E., and Wolfe, R. S. (1976) New approach to the cultivation of methanogenic bacteria: 2-mercaptoethanesulfonic acid (HS-CoM)-dependent growth of *Methanobacterium ruminantium* in a pressurized atmosphere, *Appl. Environ. Microbiol. 32*, 781−791.
15. Davis, R. W., Botstein, D., and Roth, J. R. (1980) *A Manual for Genetic Engineering: Advanced Bacterial Genetics*, Cold Spring Harbor Laboratory Press, Cold Spring Harbor, NY.
16. Inoue, H., Nojima, H., and Okayama, H. (1990) High efficiency transformation of *Escherichia coli* with plasmids, *Gene 96*, 23−28.
17. Miroux, B., and Walker, J. E. (1996) Over-production of proteins in *Escherichia coli*: mutant hosts that allow synthesis of some membrane proteins and globular proteins at high levels, *J. Mol. Biol. 260*, 289−298.
18. Tartof, K., and Hobbs, C. (1987) Improved media for growing plasmid and cosmid clones, *Bethesda Research Laboratories Focus 9*, 19.
19. Hauser, H. (2000) Short-chain phospholipids as detergents, *Biochim. Biophys. Acta 1508*, 164−181.
20. Kessi, J., Poiree, J. C., Wehrli, E., Bachofen, R., Semenza, G., and Hauser, H. (1994) Short-chain phosphatidylcholines as superior detergents in solubilizing membrane proteins and preserving biological activity, *Biochemistry 33*, 10825−10836.
21. Laemmli, U. K. (1970) Cleavage and structural proteins during the assembly of the head of bacteriophage T4, *Nature 227*, 680−685.
22. Sasse, J. (1991) Detection of Proteins, in *Current Protocols in Molecular Biology* (Ausubel, F. A., Brent, R., Kingston, R. E., Moore, D. D., Seidman, J. G., Smith, J. A., and Struhl, K., Eds.) pp 10.6.1−10.6.8, Wiley-Interscience, New York.
23. Bradford, M. M. (1976) A rapid and sensitive method for the quantitation of microgram quantities of protein utilizing the principle of protein-dye binding, *Anal. Biochem. 72*, 248−255.

24. Francis, R. T., Jr., and Becker, R. R. (1984) Specific indication of hemoproteins in polyacrylamide gels using a double-staining process, *Anal. Biochem. 136*, 509−514.
25. Dutton, P. L. (1978) Redox potentiometry: determination of midpoint potentials of oxidation-reduction components of biological electron-transfer systems, *Methods Enzymol. 54*, 411−435.
26. Gadsby, P. A., and Thomson, A. J. (1989) Assignment of the axial ligands of ferric ion in low-spin hemoproteins by near-infrared magnetic circular dichroism and electron paramagnetic resonance spectroscopy, *J. Am. Chem. Soc. 112*, 5003−5011.
27. Cammack, R., Patil, D. S., and Fernandez, V. M. (1985) Electron-spin-resonance/electron-paramagnetic-resonance spectroscopy of iron-sulphur enzymes, *Biochem. Soc. Trans. 13*, 572−578.
28. Tsou, C. L. (1951) On the cyanide inactivation of succinic dehydrogenase and the relation of succinic dehydrogenase to cytochrome b, *Biochem. J. 49*, 512−520.
29. Graham, G., Nairn, R. S., and Bates, G. W. (1978) Polyacrylamide gel staining with Fe2+-bathophenanthroline sulfonate, *Anal. Biochem. 88*, 434−41.
30. Crane, F. L. (1977) Hydroquinone dehydrogenases, *Annu. Rev. Biochem. 46*, 439−469.
31. Guzman, L. M., Belin, D., Carson, M. J., and Beckwith, J. (1995) Tight regulation, modulation, and high-level expression by vectors containing the arabinose PBAD promoter, *J. Bacteriol. 177*, 4121−4130.

BI7006564